

SLOAN DIGITAL SKY SURVEY MULTICOLOR OBSERVATIONS OF GRB 010222

BRIAN C. LEE,¹ DOUGLAS L. TUCKER,¹ DANIEL E. VANDEN BERK,¹ BRIAN YANNY,¹ DANIEL E. REICHART,²
JENNIFER ADELMAN,¹ BING CHEN,^{3,4} MIKE HARVANEK,⁵ ARNE HENDEN,⁶ ŽELJKO IVEZIĆ,⁷ SCOT KLEINMAN,⁵ DON LAMB,⁸
DAN LONG,⁵ RUSSET McMILLAN,⁵ PETER R. NEWMAN,⁵ ATSUKO NITTA,⁵ POVILAS PALUNAS,⁹ DONALD P. SCHNEIDER,¹⁰
STEPH SNEDDEN,⁵ DON YORK,^{8,11} JOHN W. BRIGGS,¹² J. BRINKMANN,⁵ ISTVAN CSABAI,^{3,13} GREG S. HENNESSY,¹⁴
STEPHEN KENT,¹ ROBERT LUPTON,⁷ HEIDI JO NEWBERG,¹⁵ AND CHRIS STOUGHTON¹

Received 2001 April 10; accepted 2001 June 22

ABSTRACT

The discovery of an optical counterpart to GRB 010222 (detected by *BeppoSAX*) was announced 4.4 hr after the burst by Henden. The Sloan Digital Sky Survey's 0.5 m photometric telescope (PT) and 2.5 m survey telescope were used to observe the afterglow of GRB 010222 starting 4.8 hr after the gamma-ray burst. The 0.5 m PT observed the afterglow in five 300 s g^* -band exposures over the course of half an hour, measuring a temporal decay rate in this short period of $F_\nu \propto t^{-1.0 \pm 0.5}$. The 2.5 m camera imaged the counterpart nearly simultaneously in five filters (u^* , g^* , r^* , i^* , z^*), with $r^* = 18.74 \pm 0.02$ at 12:10 UT. These multicolor observations, corrected for reddening and the afterglow's temporal decay, are well-fitted by the power law $F_\nu \propto \nu^{-0.90 \pm 0.03}$ with the exception of the u^* -band UV flux which is 20% below this slope. We examine possible interpretations of this spectral shape, including source extinction in a star-forming region.

Subject heading: gamma rays: bursts

1. INTRODUCTION

Gamma-ray bursts (GRBs) were first detected over three decades ago by the *Vela* satellites (Klebesadel et al. 1973), and the first search for optical counterparts started nearly immediately with W. A. Wheaton's use of the Prairie

Network (Grindlay & Wright 1974). These searches were fruitless until very recently; positions accurate to a few arcminutes were not available for days, after the bursts had decayed substantially, placing afterglows beyond the reach of the few large telescopes searching for them. BATSE's near-real-time coordinates had several degree positional errors (Paciesas et al. 1999) allowing only specialized wide field instruments to respond to its triggers (Krimm, Vanderspek, & Ricker 1995; Lee et al. 1997; Akerlof et al. 1999). The *BeppoSAX* satellite (Scarsi 1993) was the first to provide arcminute accuracy within a few hours of a GRB. With the early announcements of those accurate positions, beginning in 1997, large telescopes could join the search and discovered GRB afterglows starting with GRB 970228 (Groot et al. 1997; van Paradijs et al. 1997).

The following work describes observations of GRB 010222 with the Sloan Digital Sky Survey's (SDSS; York et al. 2000) telescopes. The SDSS is a project to image 10,000 deg² of the Northern Galactic Cap in five different filters (u^* , g^* , r^* , i^* , z^*) to a depth of $r^* \sim 23$ and to perform follow-up spectroscopy of the 10⁶ brightest galaxies and 10⁵ quasars found in the photometry. The SDSS is designed to be on the u' , g' , r' , i' , z' photometric system described in Fukugita et al. (1996) which is an AB system where flat spectrum objects ($F_\nu \propto \nu^0$) have zero colors (Fukugita et al. 1996). The magnitudes in this paper are quoted on the preliminary u^* , g^* , r^* , i^* , z^* system which may differ by at most a few percent from the system of Fukugita et al. (1996). The dedicated survey instruments, a 2.5 m survey telescope and a 0.5 m photometric telescope (PT), are located at Apache Point Observatory (APO) in Sunspot, New Mexico.

2. OBSERVATIONS

GRB 010222 was detected by *BeppoSAX* on 2001 February 22 at 07:23:30 UT in both the Gamma Ray Burst Monitor (GRBM; 40–700 keV) and the Wide Field Camera Unit 1 (WFC1; 2–28 keV) instruments and was “possibly the brightest (GRB) ever observed by *BeppoSAX*” (Piro

¹ Experimental Astrophysics Group, Fermi National Accelerator Laboratory, P.O. Box 500, Batavia, IL 60510; bcllee@fnal.gov, dtucker@fnal.gov, danvb@fnal.gov, yanny@fnal.gov, jen_a@fnal.gov, skent@fnal.gov, stoughto@fnal.gov.

² Palomar Observatory, 105-24, California Institute of Technology, Pasadena, CA 91125; der@astro.caltech.edu.

³ Department of Physics and Astronomy, Johns Hopkins University, 3701 San Martin Drive, Baltimore, MD 21218; csabai@pha.jhu.edu.

⁴ XMM Science Operation Center, European Space Agency–Vilspa, Villafranca del Castillo, Apartado 50727, 28080 Madrid, Spain; bchen@xmm.vilspa.esa.es.

⁵ Apache Point Observatory, P.O. Box 59, Sunspot, NM 88349-0059; harvanek@apo.nmsu.edu, sjk@apo.nmsu.edu, long@apo.nmsu.edu, mcmillan@apo.nmsu.edu, prn@apo.nmsu.edu, ank@apo.nmsu.edu, snedden@apo.nmsu.edu, brinkmann@nmsu.edu.

⁶ Universities Space Research Association / US Naval Observatory, Flagstaff Station, P.O. Box 1149, Flagstaff, AZ 86002-1149; aah@nofs.navy.mil.

⁷ Princeton University Observatory, Peyton Hall, Princeton, NJ 08544-1001; ivezic@astro.princeton.edu, rhl@astro.princeton.edu.

⁸ Department of Astronomy and Astrophysics, University of Chicago, 5640 South Ellis Avenue, Chicago, IL 60637; lamb@pion.uchicago.edu, don@odddjob.uchicago.edu.

⁹ Catholic University of America, NASA/Goddard Space Flight Center, Code 681, Greenbelt, MD 20771; palunas@etendue.gsfc.nasa.gov.

¹⁰ Astronomy and Astrophysics Department, Pennsylvania State University, 525 Davey Laboratory, University Park, PA 16802; dps@astro.psu.edu.

¹¹ Enrico Fermi Institute, University of Chicago, 5640 South Ellis Avenue, Chicago, IL 60637.

¹² Yerkes Observatory, University of Chicago, 373 West Geneva Street, Williams Bay, WI 53191; jwb@hale.yerkes.uchicago.edu.

¹³ Department of Physics of Complex Systems, Eötvös University, Pázmány Péter sétány 1, H-1518, Budapest, Hungary.

¹⁴ US Naval Observatory, 3450 Massachusetts Avenue, NW, Washington, DC 20392-5420; gsh@cygnus.usno.navy.mil.

¹⁵ Physics Department, Rensselaer Polytechnic Institute, SC1C25, Troy, NY 12180; heidi@rpi.edu.

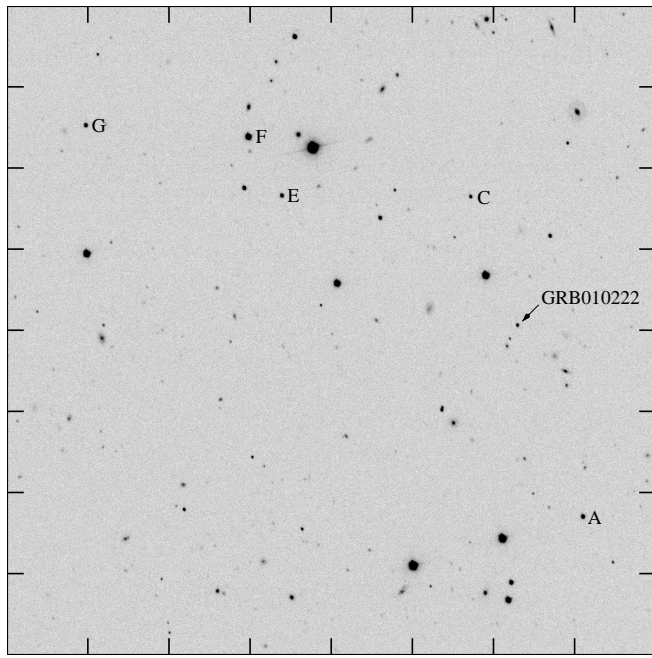


FIG. 1.—GRB 010222 2.5 m telescope r^* image. The image is 8 arcmin square with 1' tick marks. North is approximately 3° clockwise from up, east is to the left. Stars from Table 2 within this subsection of field 22 are indicated, including the reference star “A” of McDowell et al. (2001).

2001). The coordinates of the *BeppoSAX* detection were distributed via the GRB Coordinates Network (GCN; Barthelmy et al. 1998) at 10:36 UT (Piro 2001), and Henden (2001a) reported the discovery of an optical counterpart at 11:48 UT, 4.4 hr after the trigger. (See finding chart, Fig. 1.) At this time conditions at APO were not ideal for SDSS survey imaging as clouds were approaching, and the time remaining in the night did not allow for a switch to spectroscopy; thus, SDSS observers decided to follow up the counterpart with both the 0.5 m PT and the 2.5 m survey telescope. Fortunately for these observations the cloud

TABLE 1
SDSS OBSERVATIONS OF THE GRB 010222 AFTERGLOW.

UTC ^a	Telescope	Band	Exposure (s)	Magnitude ^b
12:09:35	2.5 m	r^*	54	18.74 ± 0.02
12:10:47	2.5 m	i^*	54	18.53 ± 0.02
12:11:59	2.5 m	u^*	54	19.56 ± 0.03
12:13:10	2.5 m	z^*	54	18.34 ± 0.03
12:14:22	2.5 m	g^*	54	19.02 ± 0.02
12:13:15	0.5 m	g^*	300	19.04 ± 0.04
12:19:36	0.5 m	g^*	300	19.05 ± 0.04
12:25:58	0.5 m	g^*	300	19.03 ± 0.04
12:32:19	0.5 m	g^*	300	19.10 ± 0.04
12:38:41	0.5 m	g^*	300	19.14 ± 0.04

^a Exposure start time, 2001 February 22.

^b Statistical errors: absolute photometry errors for the 2.5 m may be as large as 5% for u^* , g^* , and z^* ; 3% for r^* and i^* .

passed before GRB imaging began and conditions were more photometric after the cloud than before.

2.1. 0.5 m Photometric Telescope Observations

The photometric telescope is an f/8.8, 0.5 m telescope equipped with u^* , g^* , r^* , i^* , z^* filters. The single SITE 2048 \times 2048 CCD camera has a 41.5×41.5 field of view. The PT took a series of five 300 s observations in g^* band centered on the reported GRB 010222 location, following the afterglow for approximately 30 minutes before ending operations for the night (see Table 1). Normally, the photometric telescope and the associated reduction software are used on objects with $g^* \lesssim 18.0$. Since the GRB exposures were unusually long and the counterpart was relatively dim (the Poisson error limit is $\approx 3\%$) photometry was performed within a smaller than standard aperture to improve the relative photometry of faint objects. The counterpart magnitudes were then corrected using a sigma clipped mean of the magnitude offsets in each frame from the mean magnitude across the five frames of well-measured stars ($g^* \leq 17.0$); corrections were at most 0.005 mag, indicating conditions were photometric over the 30 minute time span.

TABLE 2
REFERENCE STARS IN THE GRB 010222 FIELD.^a

	α^b	δ^b	u^*	g^*	r^*	i^*	z^*
GRB	14 52 12.51	+43 01 06.2	19.56 ± 0.03	19.02 ± 0.02	18.74 ± 0.02	18.53 ± 0.02	18.34 ± 0.03
A	14 52 07.51	+42 58 48.6	19.39 ± 0.02	17.96 ± 0.02	17.40 ± 0.02	17.18 ± 0.01	17.08 ± 0.01
B	1452 12.57	+42 55 59.3	18.29 ± 0.02	17.02 ± 0.02	16.48 ± 0.02	16.26 ± 0.01	16.10 ± 0.01
C	14 52 16.06	+43 02 38.5	20.02 ± 0.03	19.03 ± 0.02	18.72 ± 0.02	18.61 ± 0.01	18.56 ± 0.03
D	14 52 21.86	+42 56 29.0	19.78 ± 0.03	18.42 ± 0.02	17.87 ± 0.02	17.67 ± 0.01	17.53 ± 0.02
E	14 52 28.65	+43 02 32.6	20.37 ± 0.04	18.50 ± 0.02	17.75 ± 0.02	17.45 ± 0.01	17.29 ± 0.02
F	14 52 31.09	+43 03 14.2	17.06 ± 0.01	15.89 ± 0.02	15.48 ± 0.01	15.30 ± 0.01	15.26 ± 0.01
G	14 52 41.98	+43 03 16.8	19.37 ± 0.02	18.15 ± 0.02	17.69 ± 0.02	17.52 ± 0.01	17.42 ± 0.02
H	14 52 45.90	+42 57 09.2	20.07 ± 0.04	17.80 ± 0.02	16.81 ± 0.02	16.46 ± 0.01	16.24 ± 0.01
I	14 52 50.13	+42 55 22.7	17.84 ± 0.01	16.51 ± 0.02	15.99 ± 0.01	15.83 ± 0.01	15.73 ± 0.01
J	14 52 51.32	+42 54 56.3	18.53 ± 0.02	16.49 ± 0.02	15.63 ± 0.01	15.37 ± 0.01	15.18 ± 0.01
K	14 52 51.85	+43 03 05.7	18.59 ± 0.02	16.91 ± 0.02	16.28 ± 0.01	16.01 ± 0.01	15.89 ± 0.01

NOTE.—Units of right ascension are hours, minutes, and seconds, and units of declination are degrees, arcminutes, and arcseconds.

^a Selected from stars in field 22 with magnitude $r^* \leq 19.0$ which were well measured, unsaturated, and noninterpolated (cosmic ray corrected) in all five filters, with the exception of the first star (A) in the list which is the reference star “A” listed in McDowell et al. 2001. This star was interpolated in r^* band, but manual inspection revealed no problems; the correction was small and within the quoted errors. Listed errors are statistical only, absolute photometry errors for the 2.5 m may be as large as 5% for u^* , g^* , and z^* ; 3% for r^* and i^* .

^b Because of the nonstandard orientation and short length of this stripe the astrometric errors are unusually large, approximately $0''.3$.

2.2. 2.5 m Survey Telescope Observations

The 2.5 m survey telescope is an $f/5$, 3° field of view telescope designed and constructed for the SDSS. The telescope has two interchangeable instruments, an imaging camera and a fiber-fed spectrograph. The imaging camera (Gunn et al. 1998) includes an array of 30 2048×2048 CCDs in six columns of five CCDs each, one CCD for each of the 5 filters. The camera operates in a drift scan mode, scanning the sky in great circles at sidereal rate. Astronomical objects are imaged for 53.9 s in each CCD in the order r^* , i^* , u^* , z^* , g^* . Because of the gaps between columns, the telescope must observe a second such interleaved strip to make a complete stripe.

For GRB 010222 the 2.5 m telescope observed two short interleaved strips covering a roughly 2.5 square region. The GRB 010222 counterpart was found in the second strip, field 22 of camera column 3, run 2143. The images were processed through the normal SDSS data processing pipelines and calibrated against two 0.5 m PT secondary fields (hereafter, patches) of the GRB field observed March 14 and 17. These patches in turn were calibrated against a system of standard stars (J. A. Smith et al. 2001, in preparation), which the 0.5 m PT observes several times throughout the night to measure extinction and determine photometric zero points. Our diagnostic tests of the location of the stellar locus and number counts of various classes of objects, as compared with the approximately 1000 deg^2 of sky observed already in the survey, indicate the relative calibrations are no worse than 2% in any filter. The zero points also agree to within 1% with a second indirect calibration based on other 2.5 m data from the same night and four secondary patches from two previous nights. Thus, we are confident the relative (absolute) errors are no greater than the standard SDSS values of 3% (5%) for u^* , g^* , and z^* , and 2% (3%) for r^* and i^* (where the absolute errors include possible differences between the SDSS preliminary photometric system and the system of Fukugita et al. 1996). The calibrated 2.5 m magnitudes are shown in Table 1 along with 0.5 m PT observations. Table 2 includes u^* , g^* , r^* , i^* , z^* magnitudes for eleven reference stars in field 22, including the reference star “A” listed in McDowell et al. (2001). All stars have been selected from unsaturated and noninterpolated (for cosmic ray correction) stars with $r^* \leq 19.0$, with the exception of the reference star “A” from McDowell et al. (2001). This star was interpolated in r^* band, but the correction was within the quoted errors, and visual inspection revealed no problems.

3. RESULTS

The fading of GRB optical afterglows is often well fitted by a power-law decay of $F_\nu \propto t^\alpha$ with $\alpha \approx -1$ although decay rates from slightly less than this to $\alpha = -2.1$ (Groot et al. 1998), and breaks to steeper power laws have been observed in some afterglows. GRB 010222 appears to be best-fitted by broken power-law models (Holland et al. 2001; Masetti et al. 2001) with early decay rates of $\alpha \approx -0.6$ to -0.7 and steeper later time decays of $\alpha \approx -1.3$, with the break occurring around 0.5 days after the GRB. Considering the short time span and the limiting errors, measurements of the decay rate with the 0.5 m PT observations were difficult. The error weighted least-squares fit to the five g^* points gives $\alpha = -1.0 \pm 0.5$ (see Fig. 2), which is consistent with other early decay rates measured for this burst (Price et

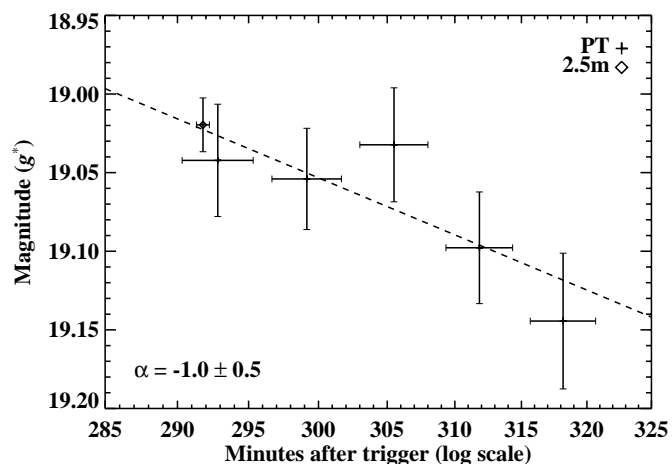


FIG. 2.—Relative photometry for five 0.5 m PT g^* -band observations, along with the single 2.5 m g^* -band observation. The best-fit decay curve of the form $F_\nu \propto t^\alpha$ to the five PT g^* -band observations is $\alpha = -1.0 \pm 0.5$.

al. 2001; Fynbo et al. 2001; Stanek et al. 2001b; Holland et al. 2001; Masetti et al. 2001).

The spectral shape of GRB afterglows is also well-fitted by a power law, $F_\nu \propto \nu^\beta$ with typical values of $\beta \approx -1$. In order to derive a power-law fit for our 2.5 m u^* , g^* , r^* , i^* , z^* observations we first corrected for the local Galactic extinction with the dust map of Schlegel, Finkbeiner, & Davis (1998), which gives extinction values of $A_{u^*} = 0.118$, $A_{g^*} = 0.087$, $A_{r^*} = 0.063$, $A_{i^*} = 0.048$, and $A_{z^*} = 0.034$ at the reported location $\alpha = 14^{\text{h}}52^{\text{m}}12^{\text{s}}55$, $\delta = +43^\circ01'06''.2$ (J2000; Henden & Vrba 2001). We next wished to correct for the small effect of fading over the few minutes between exposures in the individual bands at 4.8 hr after the burst. Because of the large errors in our own decay rate measurement we instead used a least-squares fit to a single power law for all reported R -band data points within 8 hr after the burst (and before the ≈ 0.5 day break; see McDowell et al. 2001; Stanek et al. 2001c; Watanabe et al. 2001; Holland et al. 2001) with magnitudes adjusted to the calibration of Henden (2001b), where necessary. The resulting fit to the published R -band data is $\alpha = -0.71 \pm 0.10$, consistent with values reported by Holland et al. (2001). We applied decay corrections relative to r^* of $[-0.0035, -0.0066, -0.010, -0.013]$ to i^* , u^* , z^* , and g^* .

Once these corrections were applied, the least-squares fit to all five filters is $\beta = -1.10 \pm 0.10$. However, a much better fit can be obtained by excluding the u^* filter; the remaining non-UV filters have a least-squares fit of $\beta = -0.90 \pm 0.03$ (see Fig. 3). This second value agrees closely with the spectral slope of $\beta = -0.89 \pm 0.03$ observed by Jha et al. (2001a) in a spectrum observed 4.92 hr after the burst, shortly after the 2.5 m observations. Our u^* magnitude, at an effective wavelength of 3565 \AA , is approximately 20% lower than the power-law fitted to the other bands. A similar deficit was seen in the U -band observations of Masetti et al. (2001) 1 and 2 days after the burst, and Jha et al. (2001a) may see the beginning of this steepening in their last binned spectra point near 4000 \AA . (After this work was submitted, similar U -band results were reported by Stanek et al. (2001a) for observations from 0.2 to 2 days after the burst.) These independent observations indicate this spectral feature remained constant for at least 2 days.

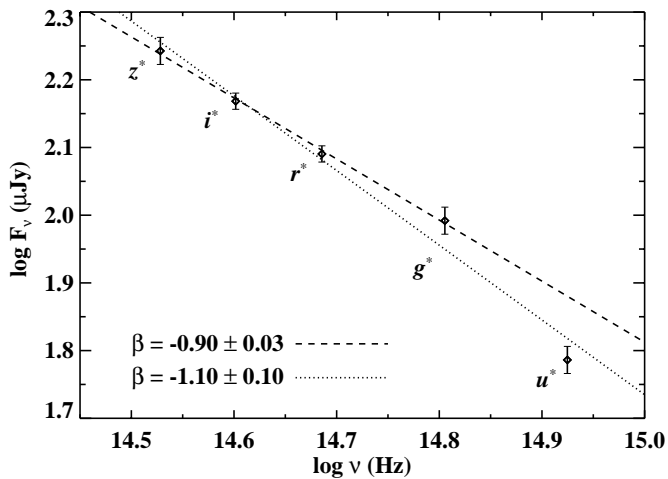


FIG. 3.—The 2.5 m multiband observations at a single epoch. The best fit to $F_\nu \propto \nu^\beta$ with all five bands is $\beta = -1.10 \pm 0.10$, shown as a dotted line. Excluding the u^* band produces a fit of $\beta = -0.90 \pm 0.03$, shown above as a dashed line.

We propose that the break in the spectrum at u^* may be an indication of one of two possibilities: either the Ly α forest or extinction at the source. The first possible explanation for the u^* deficit is that the counterpart is at a redshift near 2 rather than at the redshift 1.477 absorption system reported by Garnavich et al. (2001), Jha et al. (2001b),

Bloom et al. (2001), Castro et al. (2001), Jha et al. (2001a), and Masetti et al. (2001). For an object without detected emission lines such as GRB 010222, an absorption line system can only provide a lower z limit to the source redshift. The spectrum of Jha et al. (2001a) does not extend far past 4000 Å, thus, no upper limit is imposed until $z = 2.3$. For observed QSOs the Ly α forest enters u^* at redshifts slightly above $z = 1.477$, but the 20% depression observed here would not occur unless the redshift were $\gtrsim 2.0$ (Cristiani et al. 1993). However, Jha et al. (2001a) convincingly argue that given the strength of the $z = 1.477$ absorber the GRB source is almost certainly at that redshift. Thus, a true GRB source redshift of ≈ 2 would seem to be an unlikely explanation.

A second, more probable, explanation is that the counterpart may reside in a star-forming region at $z = 1.477$, similar to the Large Magellanic Cloud (LMC) or Small Magellanic Cloud (SMC), and be extinguished at the source. Dust in front of the GRB could cause the extinction of the afterglow and the gas would explain the large equivalent widths in the $z = 1.477$ absorption system (York et al. 1986). To examine this possibility we have fitted the full extinction curve model of Reichart (2001) to the SDSS data. Acceptable fits can be found for a wide range of intrinsic power-law spectra (with index β'). We present two possibilities, $\beta' = -0.75$ and -0.5 . These choices for β' are motivated as follows: under the models of Sari, Piran, & Narayan (1998) and Sari, Piran, & Halpern (1999) the afterglow is described

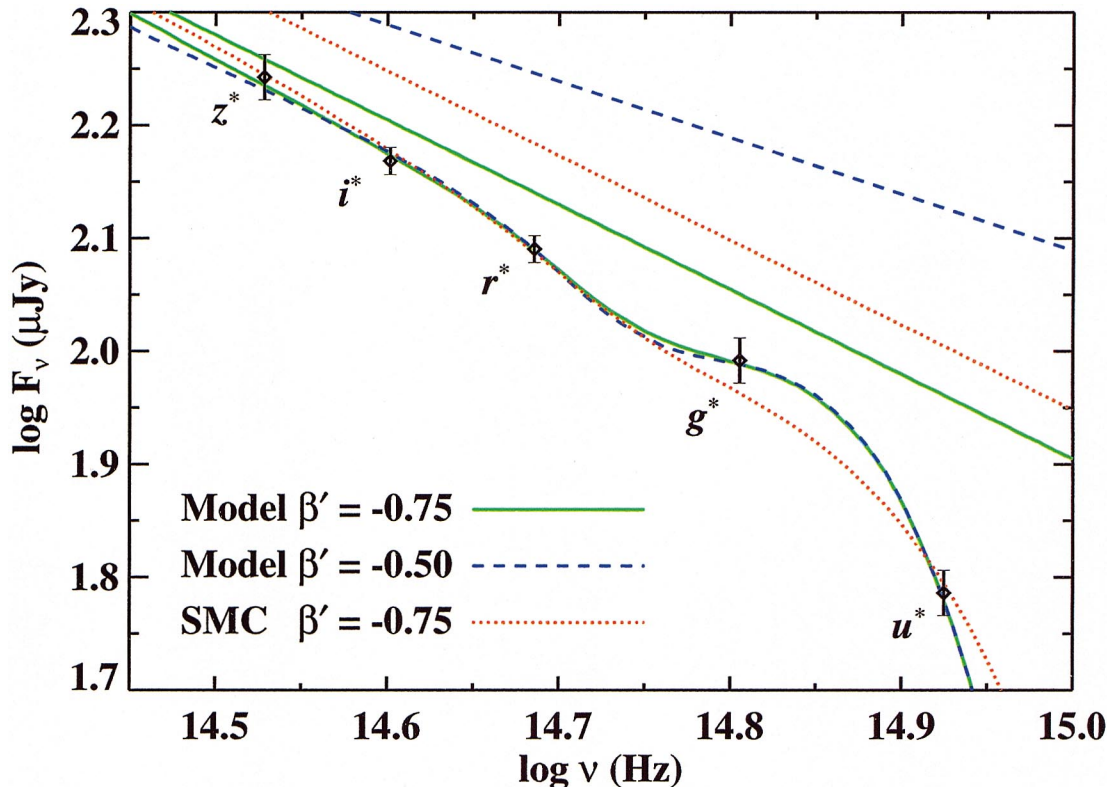


FIG. 4.—Extinction model fits to the 2.5 m multiband observations. The two best-fit extinction models from Reichart (2001) for $\beta' = -0.75$ and 0.5 , as discussed in § 3, as well as an SMC curve for an unextinguished spectrum with $\beta' = -0.75$, are presented here. The green and blue curves through the data points correspond to the Reichart (2001) extinction model fit for $z = 1.477$ and a source spectrum of $\beta' = -0.75$ (green solid curve) and $\beta' = -0.5$ (blue dashed curve). The upper lines of the same colors represent the corresponding unextinguished source spectra. The best-fit Reichart (2001) parameters for $\beta' = -0.75$ (-0.5) are a source extinction $A_V = 0.032$ (0.13), $c_2 = 1.35$ (1.34), $c_3 = 8.1$ (2.7) and $c_4 = 30$ (6.9). The dip in the curves, between r^* and g^* , is the c_3 redshifted 2200 Å bump. The steep drop through the u^* observation is the c_4 far-UV extinction (u^* samples the nonredshifted GRB spectrum from 1200 Å to 1600 Å). The upper and lower dotted red lines correspond to an unextinguished $\beta' = -0.75$ spectrum and the same spectrum extinguished by typical SMC-like extinction with $A_V = 0.10$.

in terms of synchrotron emission from a decelerating relativistic shell or jet colliding with the surrounding ISM. The resulting spectrum can be expressed as four power laws broken at three time-dependent frequencies: the synchrotron self-absorption frequency ν_a , the cooling frequency ν_c , and the frequency corresponding to the minimum Lorentz factor of accelerated electrons ν_m . If the shock evolves adiabatically in a constant density medium, the break in the light curve at ≈ 0.5 days (Holland et al. 2001; Masetti et al. 2001) might be explained by a jet if the observed $\nu_{\text{opt}} > \nu_c$ and ν_m , and $\beta' \approx -0.75$. If the shock instead evolves radiatively, the break in the light curve might be explained by ν_m passing through the optical at ≈ 0.5 days if $\nu_c < \nu_{\text{opt}} < \nu_m$, and $\beta' \approx -0.5$. For $\beta' = -0.75$ (-0.5), we find that the best fits in the Reichart (2001) model are the source extinction $A_V \approx 0.032$ (0.13) mag, the slope of the UV linear component $c_2 \approx 1.35$ (1.34), the strength of the UV bump $c_3 \approx 8.1$ (2.7), and the strength of the far-ultraviolet (FUV) nonlinear component $c_4 \approx 30$ (6.9). These curves are shown in Figure 4 which includes a typical SMC-like extinction curve for a source spectrum with $\beta' = -0.75$ and source extinction $A_V = 0.10$. For the $\beta' = -0.75$ case there is a strong degeneracy between A_V and the parameters c_3 and c_4 such that only $A_V \cdot c_3$ and $A_V \cdot c_4$ can be constrained; c_3 and c_4 can be increased to any value by decreasing A_V , thus, statistically we can only set lower bounds. For $\beta' = -0.75$, $A_V < 0.057$ mag (1 σ) and $A_V > 0$ at the 4.8 σ confidence level; $c_2 = 1.35^{+0.18}_{-0.21}$; $c_3 > 0$ at the 1.1 σ confidence level; and $c_4 > 11$ (1 σ), $c_4 > 0$ at the 2.5 σ confidence level. Further, $c_4 > 1$ (higher than any observed value) at the 2.1 σ confidence level. For $\beta' = -0.5$ the degeneracy is not as strong, and we can place the following limits: $A_V = 0.13^{+0.08}_{-0.09}$ mag and $A_V > 0$ at the 4.8 σ confidence level; $c_2 = 1.34^{+0.18}_{-0.21}$; $c_3 > 0$ at the 1.3 σ confidence level and $c_3 < 5.6$ (1 σ); $c_4 > 0$ at the 2.1 σ confidence level, $c_4 > 1$ at the 1.6 σ confidence level, and $c_4 > 3.4$ (1 σ). The Reichart (2001) fits to the two GRB models are approximately equally likely (with the $\beta' = -0.75$ model fit only 1.4 times more probable than the $\beta' = -0.5$ model fit).

The Reichart (2001) best-fit values of c_2 and the second value of c_3 are typical of that observed in the LMC. Given the errors, the first value of c_3 is not inconsistent with this interpretation. However, for both afterglow models the values of c_4 , required to extinguish u^* relative to the other bands, are about an order of magnitude greater than those found in the LMC or SMC. Waxman & Draine (2000) and Galama & Wijers (2001) propose that the optical flash (e.g., Akerlof et al. 1999) and the burst may sublimate and fragment dust in the circumburst environment. If small (radius < 300 Å) graphite grains, which may be responsible for the FUV nonlinear component (Draine & Lee 1984), survive in greater numbers in this environment, this value of c_4 is not unreasonable. Alternatively, the large c_4 value and u^* -band deficit could be due to absorption by molecular hydrogen (Draine 2000) which would span the entire u^* band at $z = 1.477$; however, the expected feature at $\lambda \leq 1650$ Å redshifted to $\lambda \approx 4000$ Å is not obvious in the published spectra.

4. CONCLUSIONS

The serendipitous 2.5 m survey telescope observations of GRB 010222 occurred in this case because of the very fortunate timing of a counterpart discovery announcement towards the end of a night when conditions did not favor normal survey operations. The 2.5 m camera is an unwieldy instrument for rapid follow-up observations; nonetheless, this observation has shown the value of early five filter observations. In addition to the measurement of the g^* , r^* , i^* , z^* spectral slope ($F_\nu \propto \nu^{-0.90 \pm 0.03}$), the break to a steeper slope in u^* (also seen in the U -band observations of Masetti et al. 2001 and Stanek et al. 2001a) was not predicted or seen in spectra and may indicate an alternate source redshift, source extinction in a star-forming region modified by the GRB or its progenitor, or something else entirely.

The 0.5 m PT is an automated telescope and in general much better suited for GRB follow-up observations than the 2.5 m survey telescope. In this case the same timing that was so fortunate for the 2.5 m was disadvantageous for the PT, which was only able to observe the burst near its limit and for a short period before shutting down for the night. Due to an afterglow's rapid decay, typical *BeppoSAX* delays of several hours place afterglows near the detection limit of smaller telescopes. *HETE-2*, launched in 2000 October, will soon provide $\sim 10'$ positions for GRBs within minutes of the trigger, potentially allowing telescopes such as the PT to measure both the spectral and temporal behavior of a burst in the first few hours.

We would like to thank Scott Barthelmy and everyone who has made the GCN possible, as well as the *BeppoSAX* team who provided the localization so crucial to this work. We would also like to thank Bruce Woodgate for his help in these observations.

The Sloan Digital Sky Survey (SDSS)¹⁶ is a joint project of the University of Chicago, Fermilab, the Institute for Advanced Study, the Japan Participation Group, the Johns Hopkins University, the Max-Planck-Institute for Astronomy (MPIA), the Max-Planck-Institute for Astrophysics (MPA), New Mexico State University, Princeton University, the United States Naval Observatory, and the University of Washington. Apache Point Observatory, site of the SDSS telescopes, is operated by the Astrophysical Research Consortium (ARC).

Funding for the project has been provided by the Alfred P. Sloan Foundation, the SDSS member institutions, the National Aeronautics and Space Administration, the National Science Foundation, the US Department of Energy, Monbusho, and the Max Planck Society.

¹⁶ The SDSS Web site is <http://www.sdss.org/>.

REFERENCES

- Akerlof, C., et al. 1999, *Nature*, 398, 400
- Barthelmy, S., et al. 1998, in *AIP Conf. Proc. 428, The GRB Coordinates Network (GCN): a Status Report*, ed. S. Barthelmy et al. (New York: AIP), 99
- Bloom, J. S., Djorgovski, S. G., Halpern, J. P., Kulkarni, S. R., Galama, T. J., Price, P. A., & Castro, S. M. 2001, *GCN Circ.* 989 (<http://gcn.gsfc.nasa.gov/gcn3/989.gcn3>)
- Castro, S., Djorgovski, S. G., Kulkarni, S. R., Bloom, J. S., Galama, T. J., Reichart, D. E., & Price, P. A. 2001, *GCN Circ.* 999 (<http://gcn.gsfc.nasa.gov/gcn3/999.gcn3>)
- Cristiani, S., Giallongo, E., Buson, L. M., Gouiffes, C., & La Franca, F. 1993, *A&A*, 268, 86
- Draine, B. T. 2000, *ApJ*, 532, 273
- Draine, B. T., & Lee, H. M. 1984, *ApJ*, 285, 89
- Fukugita, M., Ichikawa, T., Gunn, J. E., Doi, M., Shimasaku, K., & Schneider, D. P. 1996, *AJ*, 111, 1748
- Fynbo, J. P. U., et al. 2001, *GCN Circ.* 975 (<http://gcn.gsfc.nasa.gov/gcn3/975.gcn3>)
- Galama, T. J., & Wijers, R. A. M. J. 2001, *ApJ*, 549, L209
- Garnavich, P. M., Pahre, M. A., Jha, S., Calkins, M., Stanek, K. Z., McDowell, J., & Kilgard, R. 2001, *GCN Circ.* 965 (<http://gcn.gsfc.nasa.gov/gcn3/965.gcn3>)
- Grindlay, J. E., & Wright, R. E. 1974, *ApJ*, 192, L113
- Groot, P. J., et al. 1997, *IAU Circ.* 6584
- Groot, P. J., et al. 1998, *ApJ*, 502, L123
- Gunn, J. E., et al. 1998, *AJ*, 116, 3040
- Henden, A. 2001a, *GCN Circ.* 961 (<http://gcn.gsfc.nasa.gov/gcn3/961.gcn3>)
- . 2001b, *GCN Circ.* 987 (<http://gcn.gsfc.nasa.gov/gcn3/987.gcn3>)
- Henden, A., & Vrba, F. 2001, *GCN Circ.* 967 (<http://gcn.gsfc.nasa.gov/gcn3/967.gcn3>)
- Holland, S., Fynbo, J., Gorosabel, J., Henden, A., Hjorth, J., Jensen, B., & Pedersen, H. 2001, *GCN Circ.* 1002 (<http://gcn.gsfc.nasa.gov/gcn3/1002.gcn3>)
- Jha, S., et al. 2001a, *ApJ*, 554, L155
- Jha, S., Matheson, T., Calkins, M., Pahre, M. A., Stanek, K. Z., McDowell, J., Kilgard, R., & Garnavich, P. M. 2001b, *GCN Circ.* 974 (<http://gcn.gsfc.nasa.gov/gcn3/974.gcn3>)
- Klebesadel, R. W., Strong, I. B., & Olson, R. A. 1973, *ApJ*, 182, L85
- Krimm, H. A., Vanderspek, R. K., & Ricker, G. R. 1995, in *AIP Conf. Proc. 384, 3rd Huntsville Symp. on Gamma-Ray Bursts*, ed. C. Kouveliotou, M. F. Briggs, & G. J. Fishman (New York: AIP), 661
- Lee, B., et al. 1997, *ApJ*, 482, L125
- Masetti, N., et al. 2001, *A&A*, 374, 382
- McDowell, J., Kilgard, R., Garnavich, P. M., Stanek, K. Z., & Jha, S. 2001, *GCN Circ.* 963 (<http://gcn.gsfc.nasa.gov/gcn3/963.gcn3>)
- Paciesas, W. S., et al. 1999, *ApJS*, 122, 465
- Piro, L. 2001, *GCN Circ.* 959 (<http://gcn.gsfc.nasa.gov/gcn3/959.gcn3>)
- Price, P. A., Gal-Yam, A., Ofek, E., Yost, S., Bloom, J. S., Galama, T. J., Harrison, F., & Kulkarni, S. R. 2001, *GCN Circ.* 973 (<http://gcn.gsfc.nasa.gov/gcn3/973.gcn3>)
- Reichart, D. E. 2001, *ApJ*, 553, 235
- Sari, R., Piran, T., & Halpern, J. P. 1999, *ApJ*, 519, L17
- Sari, R., Piran, T., & Narayan, R. 1998, *ApJ*, 497, L17
- Scarsi, L. 1993, *A&AS*, 97, 371
- Schlegel, D. J., Finkbeiner, D. P., & Davis, M. 1998, *ApJ*, 500, 525
- Stanek, K. Z., et al. 2001a, *ApJ*, in press
- Stanek, K. Z., Challis, P., Jha, S., Kilgard, R., McDowell, J., & Garnavich, P. M. 2001b, *GCN Circ.* 983 (<http://gcn.gsfc.nasa.gov/gcn3/983.gcn3>)
- Stanek, K. Z., Jha, S., McDowell, J., Kilgard, R., Roll, J., Garnavich, P. M., & Kaluzny, J. 2001c, *GCN Circ.* 970 (<http://gcn.gsfc.nasa.gov/gcn3/970.gcn3>)
- van Paradijs, J., et al. 1997, *Nature*, 386, 686
- Watanabe, J., Kinoshita, D., Fuse, T., Komiyama, Y., Fujihara, G., Potter, B., & Harasawa, S. 2001, *GCN Circ.* 993 (<http://gcn.gsfc.nasa.gov/gcn3/993.gcn3>)
- Waxman, E., & Draine, B. T. 2000, *ApJ*, 537, 796
- York, D. G., et al. 2000, *AJ*, 120, 1579
- York, D. G., Dopita, M., Green, R., & Bechtold, J. 1986, *ApJ*, 311, 610